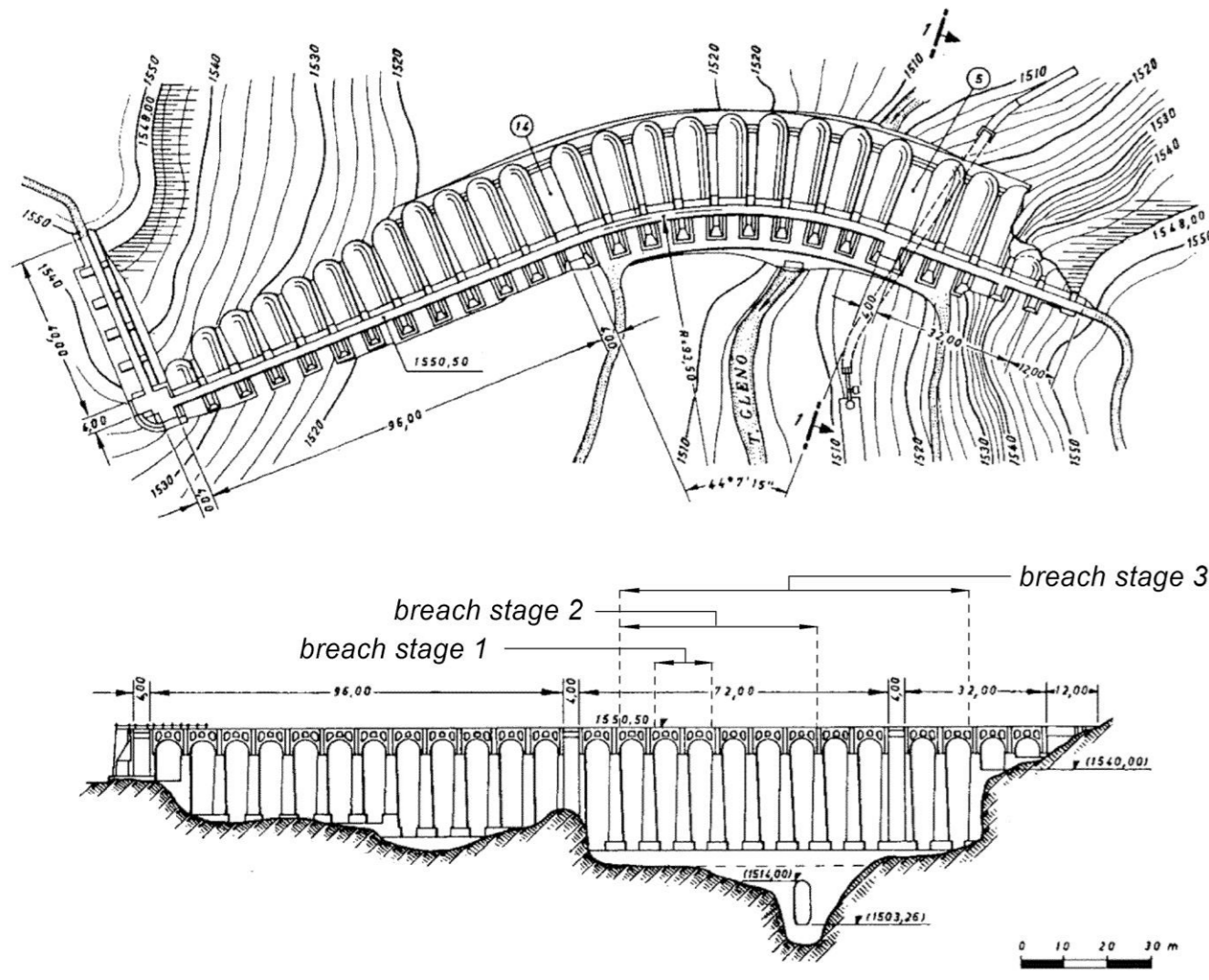


Hydraulic reconstruction of the Gleno dam break : 1 December 1923

Marco Pilotti, Massimo Tomirotti and Giulia Valerio



Plan and elevation views of the Gleno dam (modified from ANIDEL 1953). According to an eyewitness, the collapse of the dam buttresses was very rapid and happened in three stages. The eleventh spur fell first along with the two arches resting on it, causing a breach whose width can be estimated to be about 14 m. Shortly after the spur numbers 8 to 12 fell widening the breach to 48 m. Eventually, also the spurs numbered from 4 to 7 fell causing an overall final breach width of 80 m (see solid lines 1, 2 and 3 of overlying Figure). The emptying time of the reservoir was estimated to be 12–15 minutes

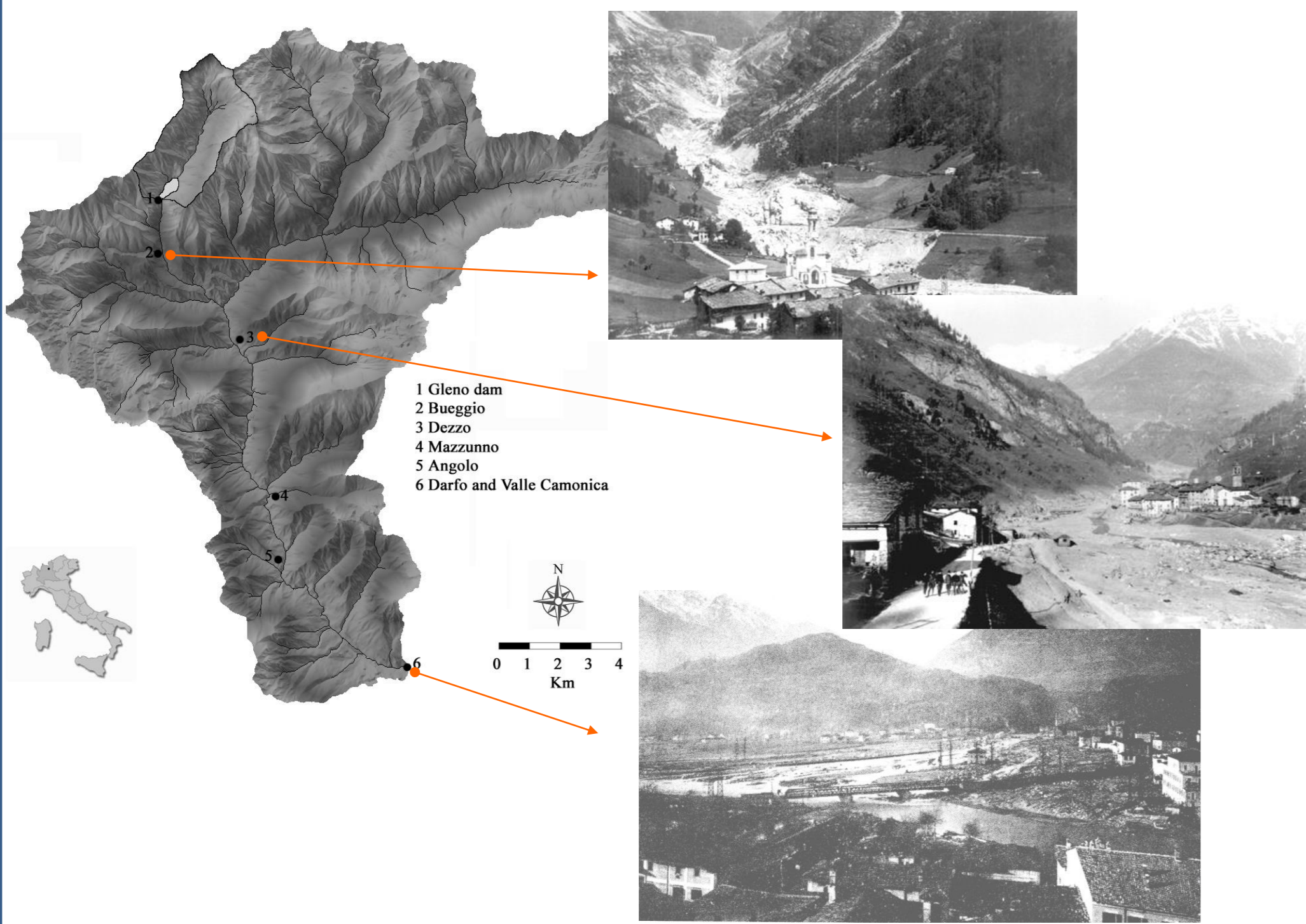
1. THE GLENO DAM-BREAK

On the morning of December 1st, 1923 the Gleno dam suddenly collapsed, about 40 days after the first complete reservoir filling. Nearly $4.5 \times 10^6 \text{ m}^3$ of water was released. As the subsequent technical examinations proved, the collapse was triggered by water seepage at the interface between the masonry base and the overlying structure. The effects of the flood propagation along the downstream river were catastrophic. The flood wave took about 45 minutes to flush the nearly 21 km long valley downstream of the dam as far as Darfo, killing nearly 400 people. The flood destroyed three villages, five power stations, and finally a high number of isolated buildings and factories. This failure is the only historical case of dam-break caused by structural deficiencies that has occurred in Italy. As a result, it has deeply influenced the evolution of Italian regulations regarding dam design. However, in spite of its relevance, this event has never been characterized from an hydraulic standpoint.



The Gleno dam a few days before the failure and the remains of the dam with the breach a few days after

2. NUMERICAL MODELLING OF RESERVOIR EMPTYING AND FLOOD PROPAGATION



Since the breach evolution is reasonably well identified, we have evaluated the outflow hydrograph by simulating the reservoir emptying. Although the outflow process following a dam break presents strongly 3-dimensional features in the neighbourhood of the breach, an effective approximation of the process is obtained by using 2-D SWE (Shallow Water Equations), according to the assumption of hydrostatic pressure distribution in the vertical. SWEs were solved using a numerical code implementing the MacCormack finite difference scheme.

$$\mathbf{U}_t + \mathbf{E}_x + \mathbf{F}_y = \mathbf{S}$$

$$\mathbf{U} = \begin{pmatrix} h \\ uh \\ vh \end{pmatrix}, \quad \mathbf{E} = \begin{pmatrix} uh \\ u^2h + \frac{1}{2}gh^2 \\ uvh \end{pmatrix}, \quad \mathbf{F} = \begin{pmatrix} vh \\ uvh \\ v^2h + \frac{1}{2}gh^2 \end{pmatrix}$$

$$\mathbf{S} = \begin{pmatrix} 0 \\ gh(S_{0x} - S_{fx}) \\ gh(S_{0y} - S_{fy}) \end{pmatrix}, \quad S_{fx} = \frac{n^2 u \sqrt{u^2 + v^2}}{h^{4/3}}, \quad S_{fy} = \frac{n^2 v \sqrt{u^2 + v^2}}{h^{4/3}}$$

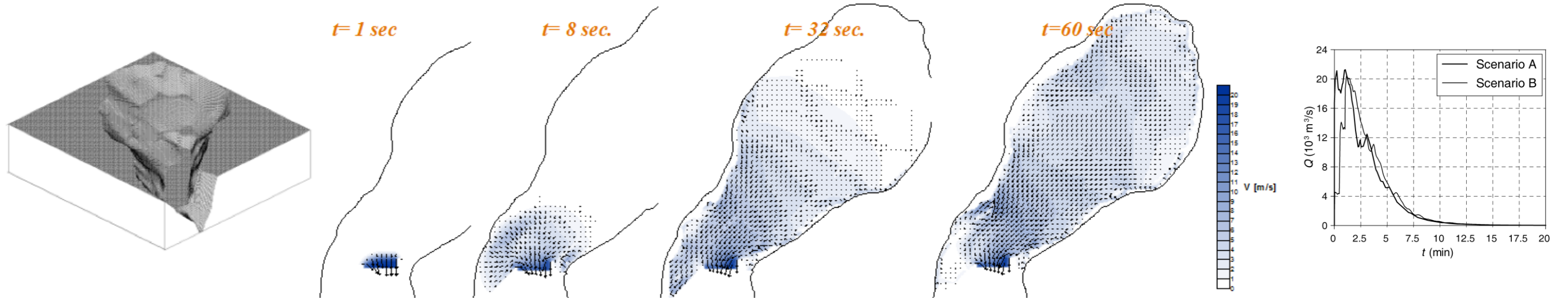
On the left, 2D Shallow Water Equations (SWE) written in a conservative vectorial form. S_0 is the bed slope and S_f the friction slope.

Below, governing equations for MacCormack method (e.g., Fennema & Chaudhry, 1986). This numerical scheme is second-order accurate, explicit and shock-capturing. It is based on a two steps predictor-corrector methodology. In order to dampen the oscillations typical of a centered second order scheme, the artificial viscosity coefficient has been introduced.

$$\left. \begin{aligned} \mathbf{U}_{i,j}^p &= \mathbf{U}_{i,j}^k - \tau_x \delta_x^- \mathbf{E}_{i,j}^k - \tau_y \delta_y^- \mathbf{F}_{i,j}^k + \Delta t \mathbf{S}_{i,j}^k \\ \mathbf{U}_{i,j}^c &= \mathbf{U}_{i,j}^k - \tau_x \delta_x^+ \mathbf{E}_{i,j}^p - \tau_y \delta_y^+ \mathbf{F}_{i,j}^p + \Delta t \mathbf{S}_{i,j}^p \end{aligned} \right\} \mathbf{U}_{i,j}^{k+1} = \frac{1}{2} (\mathbf{U}_{i,j}^p + \mathbf{U}_{i,j}^c) + \mathbf{D}_x \mathbf{U}^k + \mathbf{D}_y \mathbf{U}^k$$

$$\mathbf{D}_x \mathbf{U} = \varepsilon_{x+1/2,j} (\mathbf{U}_{i+1,j} - \mathbf{U}_{i,j}) - \varepsilon_{x-1/2,j} (\mathbf{U}_{i,j} - \mathbf{U}_{i-1,j})$$

$$\varepsilon_{x+1/2,j} = \alpha \max(v_{x,j}, v_{x+1,j}), \quad v_{x,j} = \frac{|\eta_{i+1,j} - 2\eta_{i,j} + \eta_{i-1,j}|}{|\eta_{i+1,j}| + |2\eta_{i,j}| + |\eta_{i-1,j}|}$$



Above: Reservoir bathymetry, evolution of water surface within the lake after the collapse and discharge hydrograph at the breach for the cases of sudden failure (Scenario A) and collapse duration of 1 min (Scenario B)

To model the flood propagation in the valley, we have adopted a 1D schematisation of SWE, suggested by the valley geometry with respect to the involved discharges. The classical formulation of SWE presents some problems when the bathymetry of natural valleys is irregular. Therefore, an accurate estimate of the terms S_0 and I_2 is arduous. In order to overcome these difficulties, Capart et al. (2003) proposed an approximate evaluation of the pressure force acting on wetted lateral and bottom boundary surface. It follows a modified form of SWE in which the geometric source term is written in divergence form: bottom slope and non-prismaticity effects are no longer considered geometric forcing terms, as usual, but are transferred within the momentum flux. SWE have been solved with a finite volume approach. The adopted numerical scheme is shock-capturing and capable of dealing with continuous transcritical transitions. It exactly preserves the static condition even on irregular topographies (C-property). Nevertheless, this scheme requires a very fine computational mesh in the presence of a steep water surface slope combined with steep bathymetry.

$$\frac{d}{dt} \int_{x_1}^{x_2} \mathbf{U}(x,t) dx + \mathbf{F}(\mathbf{U}(x_2,t)) - \mathbf{F}(\mathbf{U}(x_1,t)) = \int_{x_1}^{x_2} \mathbf{S}(\mathbf{U}(x,t)) dx$$

$$\mathbf{U} = \begin{pmatrix} A \\ Q \end{pmatrix}, \quad \mathbf{F} = \begin{pmatrix} \frac{Q^2}{A} + gI_1 \\ 0 \end{pmatrix}, \quad \mathbf{S} = \begin{pmatrix} 0 \\ gA(S_0 - S_f) + gI_2 \end{pmatrix}$$

$$I_1 = \int_0^{h(x,t)} (h-\eta) b(x,\eta) d\eta, \quad I_2 = \int_0^{h(x,t)} (h-\eta) \frac{\partial b}{\partial x} d\eta$$

$$\mathbf{U}_i^{n+1} = \mathbf{U}_i^n - \frac{\Delta t}{\Delta x_i} (\mathbf{f}_{i+1/2}^n - \mathbf{f}_{i-1/2}^n) + \Delta t \mathbf{S}_i^n$$

$$\begin{cases} Q_{i+1/2}^* = Q_i^n - c_{i+1/2}^* \frac{c_{i+1/2}^* - c_i^*}{4} (A_i^n - A_{i+1}^n) \\ \Sigma_{i+1/2}^{*np} = \frac{(Q_i^n)^2}{A_i^n} \\ \Sigma_{i+1/2}^{*sp} = \frac{(Q_i^n)^2}{A_i^n} + g(I_1)_i^n - g(I_1)_{i+1}^n \end{cases}$$

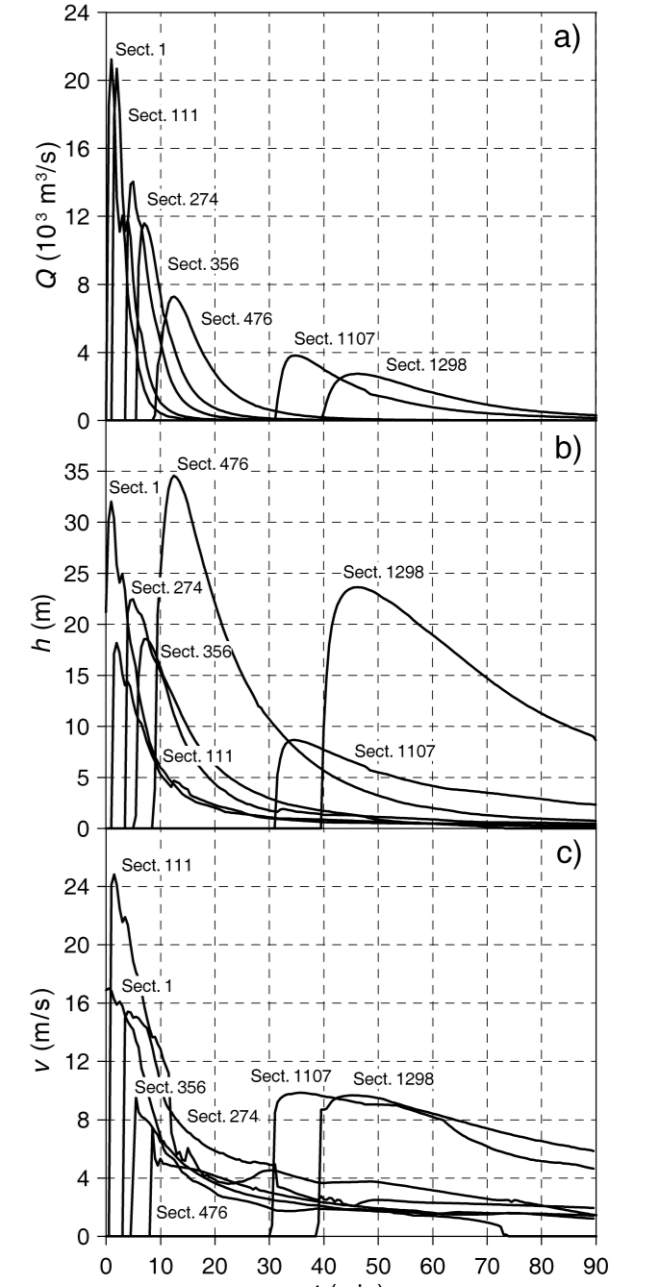
$$\begin{cases} Q_{i+1/2}^{*np} = \frac{1 + Fr_{i+1/2}^{*np}}{2} Q_i^n + \frac{1 - Fr_{i+1/2}^{*np}}{2} Q_{i+1}^n + \frac{c_{i+1/2}^* - c_i^*}{4} [1 - (Fr_{i+1/2}^{*np})^2] (A_i^n - A_{i+1}^n) \\ \Sigma_{i+1/2}^{*np} = \frac{1 + Fr_{i+1/2}^{*np}}{2} \frac{(Q_i^n)^2}{A_i^n} + \frac{1 - Fr_{i+1/2}^{*np}}{2} \frac{(Q_{i+1}^n)^2}{A_{i+1}^n} + g(I_1)_{i+1}^n - g(I_1)_i^n \\ \Sigma_{i+1/2}^{*sp} = \frac{1 + Fr_{i+1/2}^{*sp}}{2} \frac{(Q_i^n)^2}{A_i^n} + g(I_1)_{i+1}^n - g(I_1)_i^n + \frac{1 - Fr_{i+1/2}^{*sp}}{2} \frac{(Q_{i+1}^n)^2}{A_{i+1}^n} + \frac{c_{i+1/2}^* - c_i^*}{4} [1 - (Fr_{i+1/2}^{*sp})^2] (Q_i^n - Q_{i+1}^n) \end{cases}$$

$$Fr_{i+1/2}^{*np} = (V_i^n + V_{i+1}^n) / (c_i^n + c_{i+1}^n)$$

1D de Saint-Venant equations in integral form The conserved variables A and Q represent respectively the wetted cross-sectional area and the discharge, while x indicates the distance along the thalweg and t the time variable; g is the acceleration due to gravity. The terms I_1 and I_2 denote the first moment of the wetted area with respect to the free surface and the term of non-prismaticity where h is the water depth and $b(x,h)$ is the cross-sectional width at height h on the local thalweg.

Explicit updating algorithm according to the finite volume framework for the discretized variable U_i (uniform over the i -cell Δx_i) where the superscript n denotes the n -time step, while $f_{i\pm 1/2}$ are the intercell numerical fluxes

Introducing the Froude number Fr and the celerity c , the numerical estimation of the flux vector components Q^* and Σ^* is obtained by linear discretization of characteristic and compatibility equations, according to the first order algorithm proposed by Capart et al. (2003), making use of the PFP upwind scheme suggested by Braschi and Gallati (1992).



Discharge (a), water level (b) and average flow velocity (c) time series computed at some selected cross-sections

- ✓ The numerical propagation of the Gleno dam-break wave along the whole valley was accomplished using a non-uniform mesh having 1337 cross-sections
- ✓ The 1D shallow water mathematical model, even if based on restrictive hypotheses, is capable of reproducing the main macro-scale hydraulic characteristics of the event.
- ✓ The adopted numerical scheme proves to be an effective and robust tool, but requires a very fine mesh in the presence of steep slopes.
- ✓ The dynamics and timing of the failure was very well reconstructed, along with the extent of the water flooding along the valley
- ✓ This unique test case is made available to the scientific community at the web site: http://www.ing.unibs.it/~idraulica/gleno_testcase.htm.

REFERENCES:

Pilotti, M., M. Tomirotti, G. Valerio, and B. Bacchi, Simplified Method for the Characterization of the Hydrograph following a Sudden Partial Dam Break, *J. Hydraul. Eng., ASCE*, Volume 136, Issue 10, pp. 693-704 (October 2010).
 Pilotti, M., A. Maranzoni, M. Tomirotti and G. Valerio, The 1923 Gleno dam-break: case study and numerical modeling, *J. Hydraul. Eng., ASCE*, Volume 137, 480 (2011)
 Pilotti, M., Tomirotti M., Valerio G. and Milanese L. (2013): Discussion on Experimental investigation of reservoir geometry effect on dam-break flow by A. Feizi Khankandi, A. Tahershamsi And S. Soares-Frazão, *J. Hydraulic Res.* 50(4), 2012, 376–387., *Journal of Hydraulic Research*, 51:2, 220-222
 Capart, H., Eldho, T. I., Huang, S. Y., Young, D. L., and Zech, Y. (2003). Treatment of natural geometry in finite volume river flow computations. *J. Hydraul. Eng.*, 129(5), 385–393.